

## Statistical analysis of the very quiet Sun magnetism

M. J. Martínez González, R. Manso Sainz, A. Asensio Ramos

Instituto de Astrofísica de Canarias, C/Vía Láctea s/n, 38200 La Laguna, Tenerife, Spain

Departamento de Astrofísica, Univ. de La Laguna, 38205, La Laguna, Tenerife, Spain

marian@iac.es

and

A. López Ariste

THEMIS-CNRS UPS 853, Vía Láctea S/N, 38200, La Laguna, Tenerife, Spain

Received \_\_\_\_\_; accepted \_\_\_\_\_

Submitted to the Astrophysical Journal

## **ABSTRACT**

The behavior of the observed polarization amplitudes with spatial resolution is a strong constraint on the nature and organization of solar magnetic fields below the resolution limit. We study the polarization of the very quiet Sun at different spatial resolutions using ground- and space-based observations. It is shown that 80% of the observed polarization signals do not change with spatial resolution, suggesting that, observationally, the very quiet Sun magnetism remains the same despite the high spatial resolution of space-based observations. Our analysis also reveals a cascade of spatial scales for the magnetic field within the resolution element. It is manifest that the Zeeman effect is sensitive to the microturbulent field usually associated to Hanle diagnostics. This demonstrates that Zeeman and Hanle studies show complementary perspectives of the same magnetism.

*Subject headings:* Sun: magnetic fields — Sun: atmosphere — Polarization

## 1. Introduction

The quiet Sun comprises all areas outside active regions in the solar surface, which, it turn, is formed by the network and the very quiet areas inside it, the so-called internetwork. Internetwork magnetism is characterized by an intermittent pattern of positive and negative polarities, revealing a complexity larger than the one present in active regions or even in the network. The presence of a scale cascade for bipolar regions was already suggested by Stenflo (1992). This cascade apparently goes down to the sub-arcsecond or “turbulent” field that permeates 99% of the photosphere that is not occupied by the kG flux tubes of the network. It is now clear that internetwork magnetic fields are formed by a bunch of mixed-polarity magnetic fields coexisting in a single resolution element (e.g. Sánchez Almeida et al. 1996; Lites 2002; Khomenko et al. 2003; Socas-Navarro & Lites 2004; Domínguez Cerdeña et al. 2006; Orozco Suárez et al. 2007; Martínez González et al. 2008b). However, all these works had to apply very simplistic models to answer a fundamental question: which are the strengths of internetwork magnetic fields?. This question is of paramount importance to estimate the role of the internetwork on the photospheric magnetism, specially because of the large area that it occupies.

Models used to infer physical information from the observed Zeeman signals are usually based on one (or two) magnetic atmosphere(s) embedded in a non-magnetized plasma. This strategy has allowed to put in evidence that internetwork magnetic fields have a preference for hG field strengths and suggests that the topology of the magnetic field is quasi-isotropic (Martínez González et al. 2008b,a; Asensio Ramos 2009a; Bommier et al. 2009) <sup>1</sup>.

Diagnostic techniques based on the Hanle effect model the internetwork magnetic field

---

<sup>1</sup>Note that the overabundance of horizontal fields found in Orozco Suárez et al. (2007) or Lites et al. (2008) is roughly compatible with an isotropic distribution of field vectors, in which the cosine of the inclination is uniformly distributed.

assuming that it is microturbulent (isotropic below the mean free path of line-core photons). Within this scenario, magnetic field strengths  $\sim 10$ -100 G (Stenflo 1982), and  $\sim 20$ -30 G (Faurobot et al. 2001), have been inferred. A more recent estimate (Trujillo Bueno et al. 2004), based on three-dimensional radiative transfer calculations and state-of-the-art atmospheric models finds mean field strengths as high as  $\langle B \rangle \sim 130$  G. Evidence that Hanle depolarization by a randomly oriented field is indeed at work in the quiet solar photosphere was provided by Manso Sainz et al. (2004), though without giving strong constraints on the actual value of  $\langle B \rangle$ .

Simple models favor a straightforward interpretation of the data and provide an estimate of a (non-linear) average of the distribution of field strengths in the very quiet Sun. Unfortunately, since the field is known to be organized below the resolution element, this structuring escapes to our detection. Obviously, any simplified modeling fails at extracting all the information from such a complex region of the photosphere. One should rely, instead, on a statistical description of the internetwork magnetism (e.g., Sánchez Almeida et al. 1996; Carroll & Kopf 2007; Carroll 2007).

In this letter, we aim at investigating the nature of internetwork magnetism by inferring the characteristic sizes of magnetic elements. We analyze if they are macroscopic structures, microturbulent magnetic fields, or if different spatial scales coexist in the same resolution element. The variation with the spatial resolution of the polarization amplitudes we observe with the Zeeman effect gives strong constraints to the nature and organization of these magnetic fields.

## 2. Observations

We analyze high sensitivity quiet Sun spectro-polarimetric data of the Fe I lines at 630 nm using different instruments. The spectropolarimeter (SP; Lites et al. 2001) aboard Hinode spacecraft (Kosugi et al. 2007) provides us with high spatial resolution data (0.32"). The observations consist of a time series of a fixed slit position at disk center acquired on February 27

2007. The noise level in the polarization profiles is  $2.9 \times 10^{-4}$  in terms of the continuum intensity,  $I_c$ . More details can be found in Lites et al. (2008).

Two other data sets having a spatial resolution of the order of  $1.3''$  were obtained on August 17, 2003 using the POLIS instrument (Beck et al. 2005) attached to the VTT and on July 5 2008 using the ZIMPOL (Gandorfer et al. 2004) instrument mounted at THÉMIS, both telescopes at El Teide observatory. The POLIS data consist of a map of  $33.25'' \times 42''$ , along the slit and scan directions, respectively. The integration time at each slit position was  $\sim 27$  s, which allowed a noise level in the polarization profiles of  $7 \times 10^{-5} I_c$ . Details about data reduction and the observations are given by Martínez González et al. (2008b). The ZIMPOL data consist of a time series of a small scan of a quiet solar region at disk center. The scanned region was  $73.7'' \times 5''$  along the slit and the scan direction, respectively. The spatial resolution was  $\sim 1.3''$  and the noise level in the polarization profiles is of about  $5 \times 10^{-4} I_c$  after the denoising using the procedure described by Martínez González et al. (2008b).

### 3. Analysis and discussion

We investigate how the distribution of polarization amplitudes changes with the spatial resolution following two approaches. First, we compare the Hinode data set degraded to different spatial resolutions by adding adjacent pixels. This allows us to study the very same quiet Sun region at different spatial resolutions. In spite of the lower spatial resolution, POLIS and ZIMPOL observations present a better signal-to-noise ratio, thus allowing the detection of fainter signals. In order to complete the picture, we compare all data sets, although it is fundamental to remind that each observation represents the quiet Sun at different times and in different regions of the solar surface.

The comparison of the polarization amplitudes of different data sets is not straightforward.

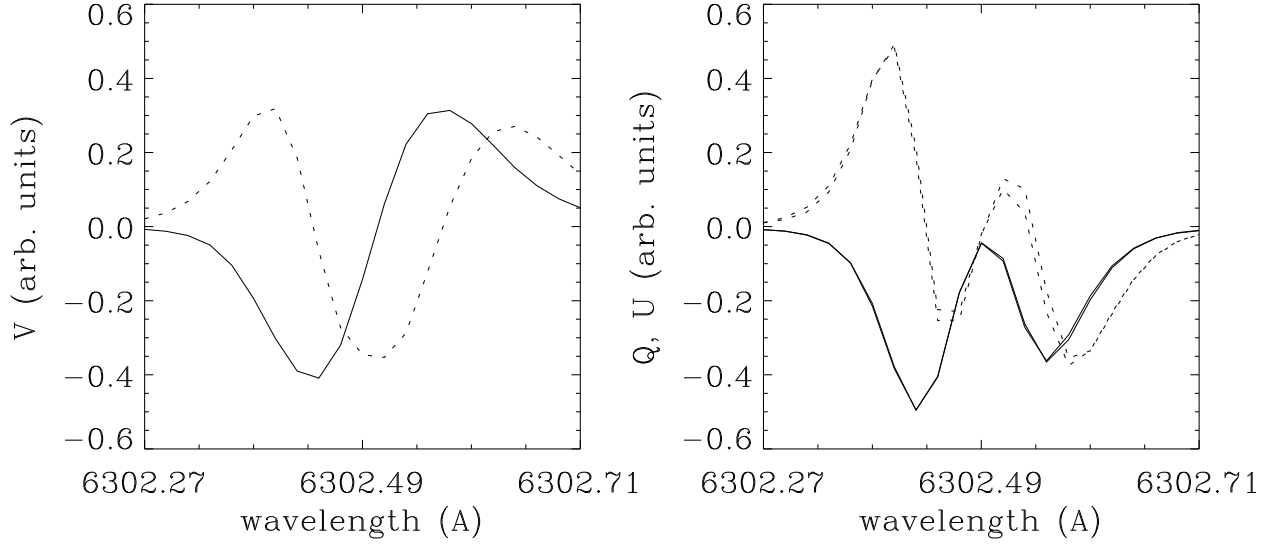


Fig. 1.— First (solid line) and second (dashed lines) principal component of the HINODE Stokes  $V$  (left panel) and  $Q$  and  $U$  (right panel) obtained from the observational data. Note the similarity between the Stokes  $Q$  and  $U$  principal components, which points towards a random distribution of azimuths in the magnetic field.

As stated in Martínez González et al. (2008a), the presence of noise introduces some systematic effects in the weak polarization tails of polarization amplitude histograms. In addition to purely instrumental errors, Stokes  $V$  profiles are affected by asymmetries in the line profile, thus making it difficult to estimate the amplitude. We propose a method based on principal component analysis (PCA) to overcome all these issues and end up with sensible comparisons between the polarization amplitudes of different data sets. Figure 1 shows the first (solid line) and second (dashed line) principal components (PC) of the Stokes  $V$  (upper panel) and Stokes  $Q$  and  $U$  (lower panel). In the case of Stokes  $V$ , the first PC (containing the vast majority of variance of the data set) is a typical antisymmetric Zeeman profile. For Stokes  $Q$  and  $U$ , the first PC is a typical symmetric Zeeman profile. The rest of the PC's contain information about velocity shifts, broadenings, asymmetries, etc. (Skumanich & López Ariste 2002). Consequently, if we describe our data sets using only the first PC, we fundamentally filter out all contributions except the one related to the amplitude of the

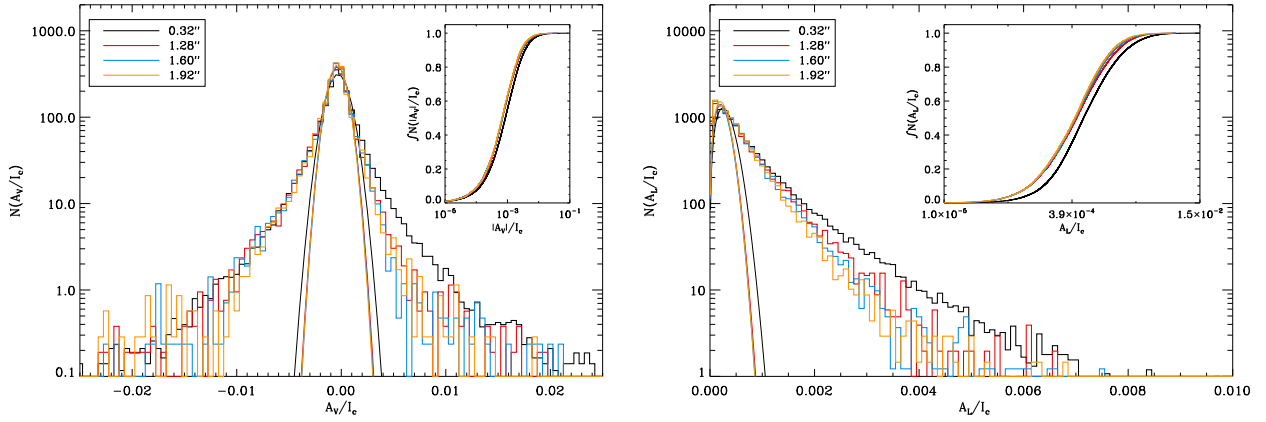


Fig. 2.— Histograms of the circular (left panel) and linear polarization (right panel) of Hinode data degraded to different spatial resolutions. The inset windows represent the empirical cumulative functions for all the histograms. Gaussian fits to the central part of the  $A_V$  histogram and the ensuing Rayleigh distributions for  $A_L$  assuming isotropy are also shown.

profiles. With this procedure, the contribution of noise and asymmetries is also strongly reduced.

The amplitude of circular polarization ( $A_V$ ) is computed as follows. We calculate the projection of the complete Stokes  $V$  data set onto the first PC. Then, since the first PC is antisymmetric, we define the amplitude of the Stokes  $V$  profiles as the semi-difference between the amplitudes of the blue and red lobes. On the other hand, the linear polarization amplitude ( $A_L$ ) is defined as the maximum value of the quantity  $(Q_1^2 + U_1^2)^{1/2}$ ,  $Q_1$  and  $U_1$  being the projection of the data set in the first PC of Stokes  $Q$  and  $U$ , respectively. Interestingly, this simple exercise allows us to extract an important conclusion from the Stokes  $Q$  and  $U$  PC's. Figure 1 shows that the first and second PC's for Stokes  $Q$  and  $U$  are nearly indistinguishable. Moreover, higher PC's having a significant variance (not shown in the figure) behave similarly. This indicates that the the azimuth of the magnetic field is uniformly distributed, with no preferred direction.

The left panel of Fig. 2 shows the histograms of  $A_V$  for Hinode data from the highest possible spatial resolution of 0.32'' down to 1.92'', obtained by direct binning of the signals. Since adding

up adjacent pixels reduces the noise of the data, we add a random noise so that all data sets at different spatial resolutions have the same noise level before computing the PC. The inset shows the empirical cumulative distribution function for  $A_V$ . The core of the circular polarization amplitude histogram changes marginally when artificially degrading the data, while the tails are more extended for the highest resolution Hinode data. This can be understood if at  $0.32''$  we are able to detect a small amount of large polarization signals that is lost for lower resolutions. Note that the histograms are plotted in log-linear scale, so that the difference detected in the tails contribute negligibly to the total area of the histogram. In particular, as seen from the cumulative distribution functions, half of the area of the histograms is contained in circular polarization amplitudes smaller than  $8.4 \times 10^{-4} I_c$  and  $6.6 \times 10^{-4} I_c$  for the  $0.32''$  and the lowest resolution data, respectively. This indicates that the median (absolute value of  $A_V$  at which we find half of the total mass of the histogram) of the Stokes  $V$  amplitudes has increased by just a factor of 1.27 when increasing the spatial resolution from  $1.92''$  to  $0.32''$ .

Regarding the linear polarization histograms, the right panel of Fig. 2 shows that the mean values are  $5.2 \times 10^{-4} I_c$  and  $4.1 \times 10^{-4} I_c$  for the  $0.32''$  and the low resolution data, respectively. Accordingly, the median linear polarization signal increases by a factor of 1.27 when increasing the spatial resolution from  $1.92''$  to  $0.32''$ .

The previous values for the median of the circular and linear polarization amplitudes indicate that the quiet Sun magnetism does not change much when increasing the spatial resolution from a few arcsec to sub-arcsec scales. We now focus on the whole shape of the histograms. First, the circular polarization amplitude histograms do not present a Gaussian shape throughout the full range of amplitudes, manifesting signatures of intermittency (e.g., Stenflo & Holzreuter 2003; Asensio Ramos 2009b). Additionally, Martínez González et al. (2008a) also found that these extended tails are modified when observing at different heliocentric angles, an indication that these tails correspond to non-isotropic structures. However, the core of

the histograms can be well reproduced by a Gaussian function. The standard deviation found for the different spatial resolutions considered are:  $\sigma_{0.32} = 1.0 \times 10^{-3} I_c$ ,  $\sigma_{1.28} = 8.6 \times 10^{-4} I_c$ , and  $\sigma_{1.60} = \sigma_{1.92} = 8.4 \times 10^{-4} I_c$ . This demonstrates that the core of the histograms at different spatial resolutions, i. e., for amplitudes between  $\pm 2.0 \times 10^{-3} I_c$  are Gaussian and almost indistinguishable. The percentage of the observed area in the Sun covered by pixels with amplitudes in the core is 77%, 82%, and 84% for the 0.32'', 1.28-1.60'' and 1.92'' data sets, respectively. A deviation from the Gaussian shape occurs for pixels with larger circular polarization amplitudes and they do display a trend with the spatial resolution. Therefore, we can state that  $\sim 20\%$  of the pixels show an increase in the magnetic flux density when increasing the spatial resolution, a consequence of the small number of signal cancellations at 0.32''.

It has been recently pointed out by Martínez González et al. (2008a) and Asensio Ramos (2009a) that the distribution of magnetic field vectors is close to isotropic in the internetwork. As a result, if the circular polarization signal and hence the longitudinal component of the magnetic field ( $B_z$ ) follows a Gaussian distribution, both  $B_x$  and  $B_y$  components necessarily follow the same distribution. The amplitude of linear polarization (as defined in this paper) under the weak field approximation is proportional to  $B_x^2 + B_y^2$  and should follow an exponential distribution. But this is true only if the fields are resolved, i.e., for individual Stokes  $Q$  and  $U$  profiles. If we assume that the signal from each resolution element is the addition of many Stokes  $Q$  and  $U$  profiles, their probability distribution should converge to a Gaussian distribution accordingly the central limit theorem. Consequently, the linear polarization signal should become close to a Rayleigh distribution. This is compatible with the drop to zero of our observational histograms. For comparison, we overplot Rayleigh distributions with modes equal to 3.5-4 times the standard deviation of the Gaussian fits for  $A_V$ . This value is in good accordance with the expected sensitivity difference for linear/circular polarization for the 630 nm lines (Martínez González et al. 2008b).

It is evident that the smaller scale magnetic elements manifesting a Gaussian behavior on the circular polarization histograms are identified with the lowest amplitudes of linear polarization. Moreover, the linear polarization histograms at different spatial resolutions behave similarly at the lowest signals, i. e., for amplitudes smaller than  $10^{-3}I_c$ . The percentage of pixels below this threshold amounts to 75% for 0.32'', 82% for 1.28'', 84% for 1.6'', and 86% for 1.92''. The non-Rayleigh tails (20% of the signals) are again more extended for the data sets with higher resolution.

We analyze in Fig. 3 the statistical properties of the polarization signals for the different observational data sets. The median of  $|A_V|$  for Hinode is a factor 1.35 larger than for ZIMPOL, while  $A_L$  is a factor 1.67 larger. Analogously, the mean unsigned flux changes a factor 2, from  $2.2 \times 10^{-3}I_c$  to  $1.0-1.1 \times 10^{-3}I_c$ , when the spatial resolution is degraded from the HINODE one to the POLIS and ZIMPOL ones. This is in agreement with the values published in the literature (see compilation in Fig. 1 of Sánchez Almeida 2009). Taking into account that the ZIMPOL data contains less observed points and that the observations are taken at different days, we reckon that the increase on polarization amplitudes is in agreement with the analysis of Hinode at different spatial resolutions. Moreover, we also behold that most of the signals are represented by a Gaussian (Rayleigh) core for circular (linear) polarization that is insensitive to spatial resolution.

These observed trends with the spatial resolution are strong constraints to the nature of the magnetic fields in the internetwork. Any proposed model for the quiet Sun magnetism should reproduce the change on the Stokes  $Q$ ,  $U$  and  $V$  amplitudes with spatial resolution. For instance, the single magnetic atmosphere surrounded by a field-free component and the simple microturbulent model are not valid models for the internetwork magnetism. The former because a single magnetic element observed at increasingly better resolutions should induce a dramatic increase in the polarimetric signal; while the latter because a microturbulent scenario is not compatible with the extended tails that evidence a cascade of spatial scales coexisting in the

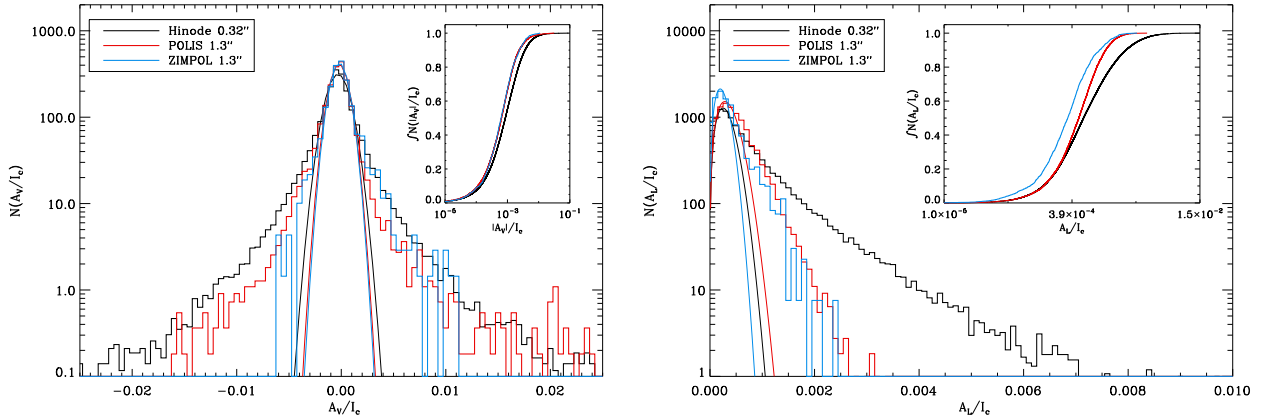


Fig. 3.— Histograms of the circular (left panel) and linear polarization (right panel) of Hinode, POLIS, and ZIMPOL data sets. The three observed data sets result in different spatial resolutions. The inset windows represent the empirical cumulative distribution functions for all the histograms. Note that, due to the peculiarities of the ZIMPOL instrument, the seeing-induced cross-talk effects are minimized with respect to the POLIS data and gives more confident data, especially when mounted at THÉMIS.

internetwork quiet Sun. The correct interpretation of the quiet Sun should take into account that the magnetic field vector  $\mathbf{B}$  depends on the scale  $r$  and the description has to rely on the complete scale-dependent continuous probability distribution function  $p(\mathbf{B}_1, r_1; \mathbf{B}_2, r_2; \dots; \mathbf{B}_n, r_n)$  (e.g., Asensio Ramos 2009b). If the scale of organization is much smaller than the resolution element, a large degree of cancellations occurs and the distribution of observed polarization amplitudes quickly tends to a Gaussian distribution. Therefore, the Gaussian core of the circular polarization amplitude histogram can be identified with the fields organized well below the resolution element. The extended tails are thus identified with magnetic elements organized at a larger scale. We calculate a “characteristic size” of the smallest magnetic elements through inversion with a model atmosphere that is formed, in each resolution element, by an isotropic distribution of magnetic field vectors all of them of the same size. With this model we get an upper limit to the size of these magnetic elements  $\sim 10$  km, which is smaller than the photon mean free path

in the photosphere. Such small scale structuring of the quiet Sun magnetism was conjectured by Sánchez Almeida et al. (1996) based on the ubiquity of the Stokes asymmetries. However, although the majority of magnetic fields in the quiet Sun is organized at such small scales, models taking into account the cascade of scales are necessary to understand the quiet Sun magnetism.

The direct analysis of observables reveals that there is not a substantial change in the polarization amplitudes from 1.3'' to 0.32''. A fraction of 80% of the circular (linear) signals follow a Gaussian (Rayleigh) distribution and seem to be insensitive to the spatial resolution. This important fact reveals that the Zeeman effect is indeed sensitive to the microturbulent magnetic field usually diagnosed with the Hanle effect. In fact, even a thousand of mixed-polarity, magnetic elements in the resolution element gives a detectable Zeeman signal (López Ariste et al. 2007). The remainder 20% of the observed polarization signals show a modification with spatial resolution, evidencing a cascade of spatial scales in the internetwork. The very quiet Sun magnetism is thus very complex and we are forced to employ sophisticated statistical modeling tools to infer its properties.

We acknowledge financial support from the Spanish MICINN through the project AYA2007-63881. Hinode is a Japanese mission developed and launched by ISAS/JAXA, with NAOJ as a domestic partner, and NASA and STFC (UK) as international partners. It is operated by these agencies in cooperation with ESA and NSC (Norway).

## REFERENCES

Asensio Ramos, A. 2009a, *ApJ*, 701, 1032

—. 2009b, *A&A*, 494, 287

Beck, C., Schmidt, W., Kentischer, T., & Elmore, D. 2005, *A&A*, 437, 1159

Bommier, V., Martínez González, M. J., Bianda, M., Frisch, H., Asensio Ramos, A., Gelly, B., & Landi Degl’Innocenti, E. 2009, *A&A*, 506, 1415

Carroll, T. A. 2007, in *Modern Solar Facilities-Advanced Solar Science*, ed. F. Kneer, K. G. Puschmann, & A. D. Wittmann, 297

Carroll, T. A., & Kopf, M. 2007, *A&A*, 468, 323

Domínguez Cerdeña, I., Sánchez Almeida, J., & Kneer, F. 2006, *ApJ*, 646, 1421

Faurobert, M., Arnaud, J., Vigneau, J., & Frisch, H. 2001, *A&A*, 378, 267

Gandorfer, A. M., Steiner, H. P. P. P., Aebersold, F., Egger, U., Feller, A., Gisler, D., Hagenbuch, S., & Stenflo, J. O. 2004, *A&A*, 422, 703

Khomenko, E. V., Collados, M., Solanki, S. K., Lagg, A., & Trujillo Bueno, J. 2003, *A&A*, 408, 1115

Kosugi, T., Matsuzaki, K., Sakao, T., Shimizu, T., Sone, Y., Tachikawa, S., Hashimoto, T., Minesugi, K., Ohnishi, A., Yamada, T., Tsuneta, S., Hara, H., Ichimoto, K., Suematsu, Y., Shimojo, M., Watanabe, T., Shimada, S., Davis, J. M., Hill, L. D., Owens, J. K., Title, A. M., Culhane, J. L., Harra, L. K., Doschek, G. A., & Golub, L. 2007, *Sol. Phys.*, 243, 3

Lites, B. W. 2002, *ApJ*, 573, 431

- Lites, B. W., Elmore, D. F., & Streater, K. V. 2001, in ASP Conf. Series, Vol. 236, *Advanced Solar Polarimetry – Theory, Observation, and Instrumentation*, ed. M. Sigwarth, 33
- Lites, B. W., Socas-Navarro, H., Berger, T., Frank, Z., Shine, R., Tarbell, T., Title, A., Ichimoto, K., Katsukawa, Y., Tsuneta, S., Suematsu, Y., Shimizu, T., & Nagata, S. 2008, *ApJ*, 672, 1237
- López Ariste, A., Malherbe, J. M., Manso Sainz, R., Asensio Ramos, A., Ramírez Vélez, J. C., & Martínez González, M. J. 2007, in SF2A-2007, ed. . C. C. J. Bouvier, A. Chalabaev, SF2A, 592
- Manso Sainz, R., Landi Degl’ Innocenti, E., & Trujillo Bueno, J. 2004, *ApJ*, 614, 89
- Martínez González, M. J., Asensio Ramos, A., López Ariste, A., & Manso Sainz, R. 2008a, *A&A*, 479, 229
- Martínez González, M. J., Collados, M., Ruiz Cobo, B., & Beck, C. 2008b, *A&A*, 477, 953
- Orozco Suárez, D., Bellot Rubio, L. R., del Toro Iniesta, J. C., Tsuneta, S., Lites, B. W., Ichimoto, K., Katsukawa, Y., Nagata, S., Shimizu, T., Shine, R. A., Suematsu, Y., Tarbell, T. D., & Title, A. M. 2007, *ApJ*, 670, 61
- Sánchez Almeida, J. 2009, *Astrophys. Space Sci.*, 320, 121
- Sánchez Almeida, J., Landi Degl’ Innocenti, E., Martínez Pillet, V., & Lites, B. W. 1996, *ApJ*, 466, 537
- Skumanich, A., & López Ariste, A. 2002, *ApJ*, 570, 379
- Socas-Navarro, H., & Lites, B. W. 2004, *ApJ*, 616, 587
- Stenflo, J. O. 1982, *Sol. Phys.*, 80, 209

Stenflo, J. O. 1992, in *Electromechanical coupling of the solar atmosphere.*, ed. D. S. Spicer & P. MacNeice, 267 (AIPC), 40–54

Stenflo, J. O., & Holzreuter, R. 2003, in *Astronomical Society of the Pacific Conference Series*, Vol. 286, *Current Theoretical Models and Future High Resolution Solar Observations: Preparing for ATST*, ed. A. A. Pevtsov & H. Uitenbroek, 169–+

Trujillo Bueno, J., Shchukina, N., & Asensio Ramos, A. 2004, *Nature*, 430, 326